Available online at www.sciencedirect.com
ScienceDirect
Catalysis Today 126 (2007) 449–455
CATALYSIS TODAY
www.elsevier.com/locate/cattod

Promotion effect of residual K on the decomposition of N_2O over cobalt–cerium mixed oxide catalyst

Li Xue [a], Changbin Zhang [a], Hong He [a,*], Yasutake Teraoka [b]

[a] *State Key Laboratory of Environmental Chemistry and Ecotoxicology, Research Center for Eco-Environmental Sciences, Chinese Academy of Sciences, Beijing 100085, China*

[b] *Department of Energy and Material Sciences, Faculty of Engineering Sciences, Kyushu University, Kasuga, Fukuoka 816-8580, Japan*

Available online 16 July 2007

Abstract

A series of cobalt–cerium mixed oxide catalysts (Co_3O_4–CeO_2) with a Ce/Co molar ratio of 0.05 were prepared by co-precipitation (with K_2CO_3 and KOH as the respective precipitant), impregnation, citrate, and direct evaporation methods and then tested for the catalytic decomposition of N_2O. XRD, BET, XPS, O_2-TPD and H_2-TPR methods were used to characterize the catalysts. Catalysts with a trace amount of residual K exhibited higher catalytic activities than those without. The presence of appropriate amount of K in Co_3O_4–CeO_2 may improve the redox property of Co_3O_4, which is important for the decomposition of N_2O. When the amount of K was constant, the surface area became the most important factor for the reaction. The co-precipitation-prepared catalyst with K_2CO_3 as precipitant exhibited the best catalytic performance because of the presence of ca. 2 mol% residual K and the high surface area. We also discussed the rate-determining step of the N_2O decomposition reaction over these Co_3O_4–CeO_2 catalysts.

Keywords: N_2O decomposition; Co_3O_4; CeO_2; Mixed oxide; Co-precipitation; O_2-TPD; H_2-TPR; Redox ability; K_2CO_3; Residual K

1. Introduction

Nitrous oxide (N_2O), commonly known as laughing gas, is now recognized as an environmental pollutant. N_2O is not only a substantial contributor to catalytic ozone depletion by being a major source of NOx in the stratosphere, but is also a greenhouse gas [1–4]. N_2O has 310 and 21 times the global warming potential (GWP) of CO_2 and CH_4, respectively [3].

N_2O is produced by both natural and anthropogenic sources. To control the emission of N_2O from chemical processes, the catalysts for N_2O decomposition have been widely studied in the last three decades; these include supported metals, transition metal ion exchanged zeolites, pure and mixed oxides [3–18]. Among them, mixed oxides containing cobalt spinel (Co_3O_4) showed the best catalytic activity in the decomposition of N_2O [4,10–18]. Calcined hydrotalcites containing cobalt, such as Co–Al–HT [11–13], Co–Mg–Al–HT [14] and Co–Rh–Al [11,14], etc., have been reported to be very efficient for the decomposition of N_2O. Yan et al. [16,17] have found that when Co^{2+} in Co_3O_4 was partially replaced by Ni^{2+}, Zn^{2+}, or Mg^{2+} the catalytic activity of cobalt spinel could be greatly improved. In our previous work [18], we prepared a series of cobalt–cerium mixed oxide catalysts (Co_3O_4–CeO_2) with different Ce/Co molar ratios using co-precipitation method (K_2CO_3 as precipitant). We found that Co_3O_4–CeO_2 catalyst with a Ce/Co molar ratio of 0.05 showed very good activity in the reaction for N_2O decomposition. The addition of an appropriate amount of CeO_2 could increase the surface area of Co_3O_4, and improve the redox ability of Co^{2+}/Co^{3+}.

In this work, five Co_3O_4–CeO_2 (mole ratio of Ce/Co equals 0.05) catalysts were prepared using co-precipitation (with K_2CO_3 and KOH as precipitant, respectively), impregnation, citrate, and direct evaporation methods, and then tested for the catalytic decomposition of N_2O. BET, X-ray powder diffraction (XRD), X-ray photoelectron spectroscopy (XPS), O_2 temperature-programmed desorption (O_2-TPD), and temperature-programmed reduction by H_2 (H_2-TPR) methods were used to characterize the catalysts. The presence of residual K in Co_3O_4–CeO_2 was found to be very important for the decomposition of N_2O.

* Corresponding author. Tel.: +86 10 62849123; fax: +86 10 62923563.
E-mail address: honghe@rcees.ac.cn (H. He).

0920-5861/$ – see front matter © 2007 Elsevier B.V. All rights reserved.
doi:10.1016/j.cattod.2007.06.021

2. Experimental

2.1. Preparation of catalysts

Co_3O_4–CeO_2 catalysts, with a Ce/Co molar ratio of 0.05, were synthesized by the following methods.

The first and second Co_3O_4–CeO_2 catalysts were synthesized by co-precipitation method with different precipitants. A solution of 1 M K_2CO_3 or KOH was added dropwise to a solution containing known amounts of $Co(NO_3)_2$ and $Ce(NO_3)_3$ at room temperature until the pH of the solution reached 9.1. The slurry was stirred for 1 h and aged for 3 h before being filtered. The precipitate obtained using K_2CO_3 as precipitant was colloidal. When using KOH as precipitant, however, the obtained precipitate was easy to be deposited from the solution during the aging process. Both resultant precipitates were washed until the pH of the filtrate was 7, dried at 100 °C overnight, and followed by calcinations at 400 °C in static air for 2 h. The catalysts obtained are referred to as CC-CP1 (K_2CO_3 as precipitant) and CC-CP2 (KOH as precipitant), respectively.

The third Co_3O_4–CeO_2 catalyst was prepared by impregnating Co_3O_4 (prepared by the precipitation method with K_2CO_3 as precipitant) with aqueous $Ce(NO_3)_3$ solution. The sample was dried at 100 °C overnight, and calcined at 400 °C for 2 h. The catalyst is referred to as CC-Im.

The fourth Co_3O_4–CeO_2 catalyst was prepared by the citrate method. $Co(NO_3)_2$ and $Ce(NO_3)_3$ in appropriate quantities were dissolved in distilled water. Citric acid monohydrate was then added to the mixture according to the stoichiometry of each reaction (citric acid/Ce = 1/1 and citric acid/Co = 2/3) under continuous stirring. Water was then removed on a rotary evaporator at 80 °C until a viscous gel was formed. The gel was dried overnight in an oven set at 100 °C, and a spongy, highly hygroscopic, amorphous precursor was obtained. The precursor was calcined at 400 °C for 2 h to obtain the mixed oxide. The catalyst prepared by this method is referred to as CC-Ct.

Finally, a Co_3O_4–CeO_2 catalyst was prepared by thermal decomposition of a mixture of metal nitrate precursors. Aqueous solutions of $Co(NO_3)_2$ and $Ce(NO_3)_3$ were mixed in appropriate quantities. The mixture was direct evaporated to dryness at 100 °C, and calcined at 400 °C in static air for 2 h. The catalyst prepared by this direct evaporation method is thus referred to as CC-DE.

2.2. Activity measurements

The catalytic reaction was carried out in a fixed-bed quartz flow reactor, containing approximately 0.5 g of catalyst in all the experiments. The reactor was heated by a temperature-controlled furnace. A thermocouple was placed on the outside of the reactor tube. Prior to the reaction all samples were pretreated for 30 min by 20% O_2 in Ar at 400 °C to yield clean surfaces, followed by cooling down to the reaction temperature in the same gas. Then a reaction mixture of N_2O (1000 ppm) in Ar was introduced into the reactor at a flow rate of 150 $cm^3\ min^{-1}$, yielding a space velocity (W/F) of 0.2 g s cm^{-3}. Analysis of the reaction products was carried out using a gas chromatograph (Agilent 6890N equipped with Porapak Q and Molecular Sieve 5A columns). The reaction system was kept for 1 h at each reaction temperature to reach a steady state before analysis of the product was performed. In all tests, N_2 and O_2 were the only gaseous products that were observed.

2.3. Characterization of catalysts

The Co_3O_4–CeO_2 catalysts' BET surface areas were measured using a Quantasorb-18 automatic equipment. The samples were characterized by X-ray diffractometry using a computerized Rigaku D/max-RB Diffractometer (Japan, Cu Kα radiation, 0.154056 nm). The step scans were taken over a range of 10–90° in step of 4° min^{-1}. The crystallite size of the solids investigated was calculated from line-broadening analysis of some diffraction lines of the Co_3O_4 phase using Scherrer equation:

$$d = \frac{K\lambda}{B_{1/2}\cos\theta}$$

where d is the mean crystallite diameter, λ the X-ray wavelength, K the Scherrer constant (0.9), $B_{1/2}$ the full-width-half-maximum (FWHM) of the Co_3O_4 diffraction peaks and θ is the diffraction angle.

The catalysts were analyzed using X-ray photoelectron spectroscopy (XPS) to identify the surface nature and concentration of the active species. Spectra were recorded by an ESCALAB Mark II spectrometer (Vacuum Generators, UK) using Al Kα radiation ($h\nu$ = 1486.6 eV) with a constant pass energy of 50 eV. Charging effects were corrected by referencing C 1s measurements at 284.6 eV.

O_2-TPD experiments were performed in a flow of He (30 $cm^3\ min^{-1}$) over 200 mg of catalyst using a heating rate of 30 °C min^{-1}. Prior to the TPD experiments, the catalysts were pretreated under a flow of 2% N_2O/Ar (or 10% O_2/He) at 400 °C for 1 h, followed by cooling down to room temperature in the same flow. The decomposition of N_2O over the catalyst would leave adsorbed oxygen species on the surface, which could be detected by a mass spectrometer (Hiden) in the TPD experiments.

Temperature-programmed reduction (TPR) experiments were performed under a flow of a 5% H_2/Ar mixture (30 $cm^3\ min^{-1}$) over 50 mg of catalyst using a heating rate of 10 °C min^{-1}. Prior to TPR, the catalysts were treated under a 20% O_2/He mixture at 400 °C for 1 h to yield clean surfaces. A mass spectrometer (Hiden) was used for on-line monitoring of the TPR effluent gas.

3. Results

3.1. Activity measurements

Catalytic activities of N_2O decomposition over Co_3O_4–CeO_2 catalysts prepared by different methods are presented in

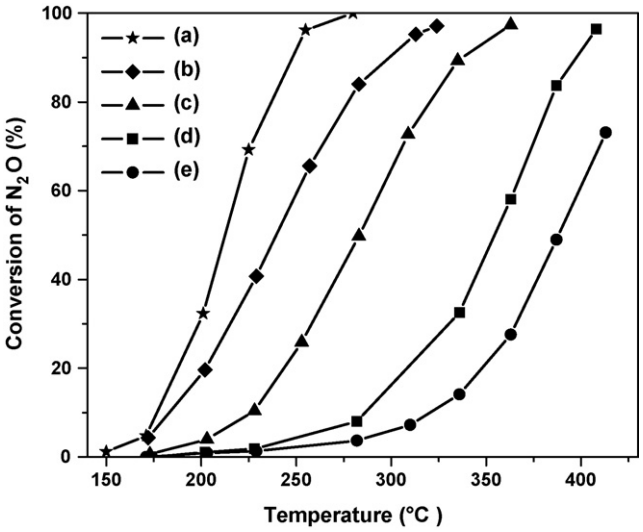

Fig. 1. Conversion of N_2O over (a) CC-CP1, (b) CC-Im, (c) CC-CP2, (d) CC-Ct, and (e) CC-DE catalysts. Conditions—total flow: 150 cm^3 min^{-1}; gas composition: 1000 ppm N_2O/Ar; weight of catalyst: 0.5 g.

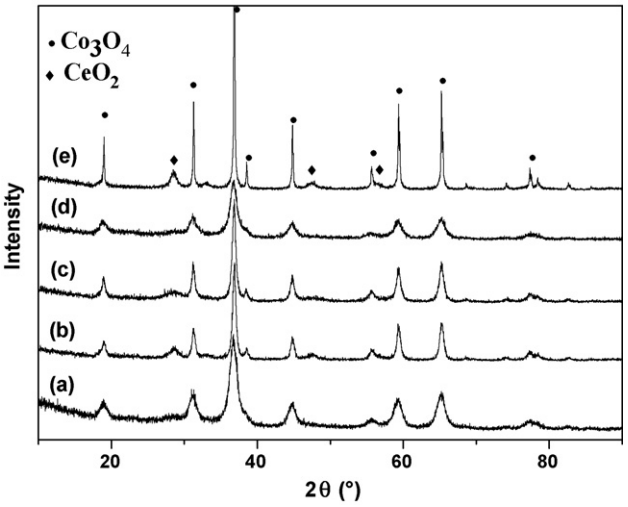

Fig. 2. XRD patterns of (a) CC-CP1, (b) CC-Im, (c) CC-CP2, (d) CC-Ct, and (e) CC-DE catalysts.

Fig. 1. It is evident that the preparation method has a strong influence on the catalytic performance. The catalyst prepared by co-precipitation method with K_2CO_3 as precipitant (CC-CP1) showed the best activity, followed by the sample prepared by the impregnation method (CC-Im). When KOH served as the precipitant the activity curve of the obtained catalyst (CC-CP2) shifted to higher temperatures compared to the CC-Im catalyst. The citrate method prepared catalyst (CC-Ct) and the direct evaporated catalysts (CC-DE) were much less active.

In an earlier study [18], we found that the addition of an appropriate amount of CeO_2 could improve the catalytic activity of Co_3O_4 in the decomposition of N_2O. The interaction between CeO_2 and Co_3O_4 was supposed to be the cause of the promotion effect. In the present work, the influence of the preparation method on the catalytic performance that we observed may also correspond to different interactions between Co_3O_4 and CeO_2. When using different preparation methods, the textural and structural properties, the chemical environment around the active site (Co^{2+}) and the redox ability of Co^{2+} may all be different. As a consequence, the catalytic activities of the Co_3O_4–CeO_2 catalysts are dramatically different from each other. In order to clarify the reason for the difference in catalytic performance, we carried out a series of experiments to characterize the catalysts.

3.2. XRD and BET

The XRD patterns of the Co_3O_4–CeO_2 catalysts prepared by different methods are present in Fig. 2. XRD reflections of cobalt spinel (Co_3O_4, JCPDS 80-1541) were present in the patterns of all the Co_3O_4–CeO_2 catalysts. The average Co_3O_4 crystallite sizes determined from the (4 4 0) peak of the diffraction ($2\theta = 65.2^\circ$) using the Scherrer equation are given in Table 1. It can be seen that the CC-DE catalyst had the largest Co_3O_4 crystallites, followed by the CC-Im and CC-CP2 catalysts, while the CC-Ct and CC-CP1 catalysts had rather small crystallites. XRD reflections of CeO_2 with a fluorite oxide-type structure (JCPDS 34-0394) were present in the patterns of the CC-DE, CC-CP2, and CC-Im catalysts. The absence of CeO_2 reflections in the CC-Ct and CC-CP1 patterns indicates that CeO_2 must exist as a highly dispersed or amorphous species in these two catalysts.

The BET surface areas of the catalysts are present in Table 1. The surface area of the catalyst correlates well with the crystallite size calculated by XRD patterns. The CC-CP1 catalyst had the largest surface area, followed by the CC-Ct, CC-CP2, and CC-Im. CC-DE catalyst, which had the largest crystallite size, had the smallest surface area in this series. However, the differences in surface area and XRD patterns were not in good agreement with those exhibited in the activity test over these Co_3O_4–CeO_2 catalysts. This result suggests that the textural and structural properties are not the main reasons for the great difference in catalytic activity over these catalysts.

3.3. XPS measurements

XPS measurements were performed on the Co_3O_4–CeO_2 catalysts to examine the valence state of Co and Ce and the surface element composition of the catalysts. The XPS spectra of Co 2p, Ce 3d, and K 2p are shown in Fig. 3. The surface

Table 1
The surface area and Co_3O_4 crystallite size of Co_3O_4–CeO_2 catalysts prepared by different methods

Catalyst	Surface area (m^2 g^{-1})	Crystallite size of Co_3O_4 (nm)
CC-CP1	106	10.7
CC-Im	57	16.3
CC-CP2	67	15.6
CC-Ct	87	11.3
CC-DE	21	44.3

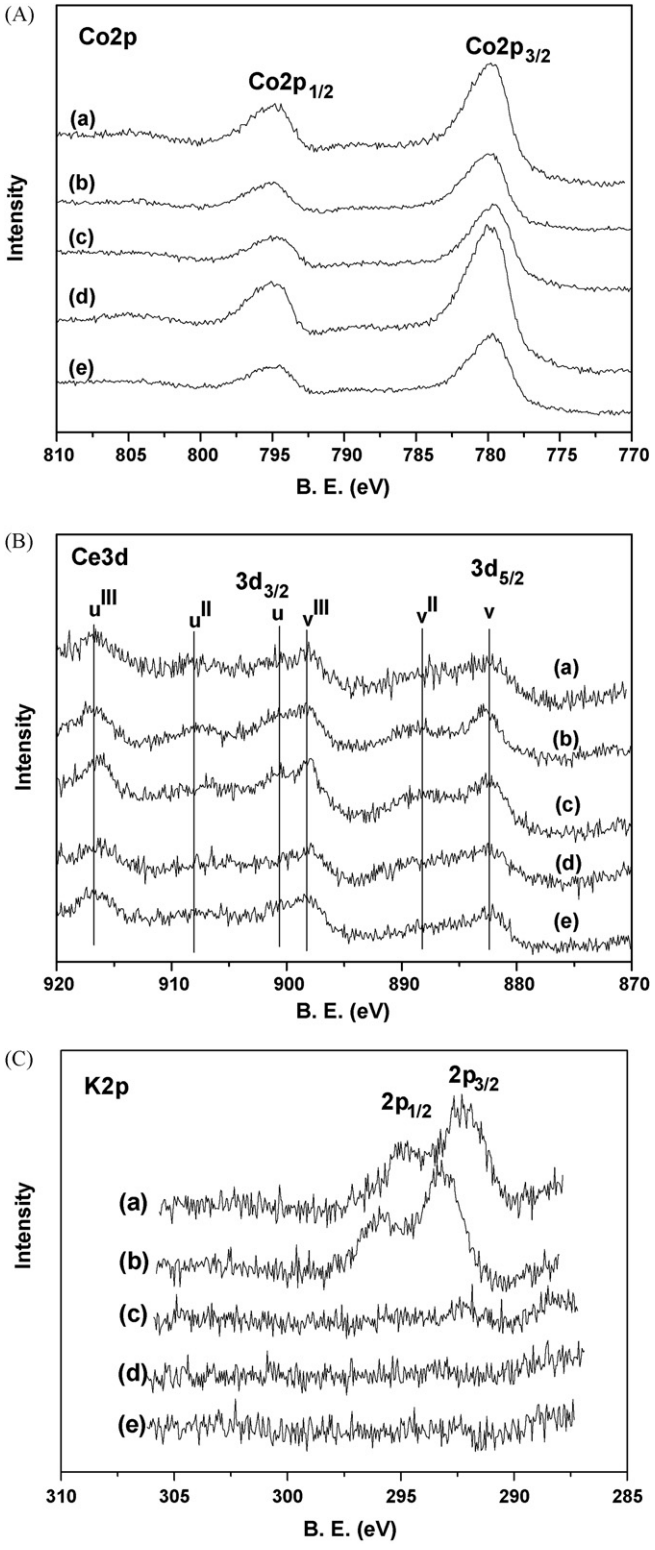

Fig. 3. XPS of Co 2p level (A), Ce 3d level (B) and K 2p level (C) for (a) CC-CP1, (b) CC-Im, (c) CC-CP2, (d) CC-Ct, and (e) CC-DE catalysts.

concentration of K and the molar ratio of Ce/Co of these catalysts are summarized in Table 2.

In Fig. 3(A), the peaks of Co $2p_{3/2}$ BE for all samples appeared at around 779.7–780.1 eV, which is in good agreement with the reference data for Co_3O_4 [19,20]. Fig. 3(B) shows the XPS spectra of Ce 3d. The three main $3d_{5/2}$ features at 882.4, 888.4, and 898.0 eV correspond to the v, v^{II}, and v^{III} components, respectively. The $3d_{3/2}$ features at 900.3, 906.9, and 916.3 eV correspond to the u, u^{II}, and u^{III} components, respectively. These three pairs of peaks arise from different Ce 4f electron configurations in the final states of the Ce^{4+} species [21–23]. There is not a great difference in the valence state of cobalt and cerium in these catalysts prepared by different methods. The surface molar ratios of Ce/Co measured by XPS are present in Table 2. This result showed that the surface Ce/Co molar ratios were apparently higher than the corresponding nominal value (0.05), suggesting a preference of ceria segregating on the surface. However, the surface molar ratios of Ce/Co were different when using different preparation methods. The CC-Im catalyst had the highest Ce/Co ratio followed by the CC-CP2 and CC-DE catalysts. The CC-Ct and CC-CP1 catalysts had the lowest surface molar ratio of Ce/Co = 0.1.

Table 2
The surface composition of Co_3O_4–CeO_2 catalysts prepared by different methods

Catalyst	Ce/Co molar ratio	K (mol%)
CC-CP1	0.10	1.9
CC-Im	0.23	2.3
CC-CP2	0.21	0.7
CC-Ct	0.10	–
CC-DE	0.17	–

In Fig. 3(C), the peaks of K 2p BE of all samples are present. There was ca. 2 mol% residual K presented on the CC-CP1 and CC-Im catalysts (Co_3O_4 was prepared by precipitation method with K_2CO_3 as precipitant) in the XPS measurement. The residual K on the CC-CP2 catalyst was about 0.7 mol%. It was noteworthy that all catalysts containing K showed higher catalytic activities than those without K.

3.4. O_2-TPD measurements

The decomposition of N_2O is reported to proceed by an oxidation–reduction mechanism [4]. Transition metal ions with more than one valence often act as the active site in this reaction. In the case of the Co_3O_4–CeO_2 catalysts, Co^{2+} in Co_3O_4 serves as the active site (Eqs. (1) and (2)). The desorption of adsorbed oxygen (Eq. (2)) has been reported to be the rate-determining step of the whole reaction over a cobalt spinel catalyst [4,10]. Therefore, we performed O_2-TPD experiments over these Co_3O_4–CeO_2 catalysts pretreated with N_2O to study their O_2 desorption behavior.

$$N_2O + Co^{2+} \rightarrow N_2 + Co^{3+}{-}O^{-} \quad (1)$$

$$2Co^{3+}{-}O^{-} \rightarrow O_2 + 2Co^{2+} \quad (2)$$

Prior to the TPD experiment, the catalysts were pretreated under a flow of 2% N_2O/Ar at 400 °C for 1 h, followed by cooling down to room temperature in the same flow. Adsorbed oxygen species, derived from the decomposition of N_2O, would be left on the catalyst if the temperature of O_2 desorption is higher than that of N_2O decomposition. Fig. 4 shows the

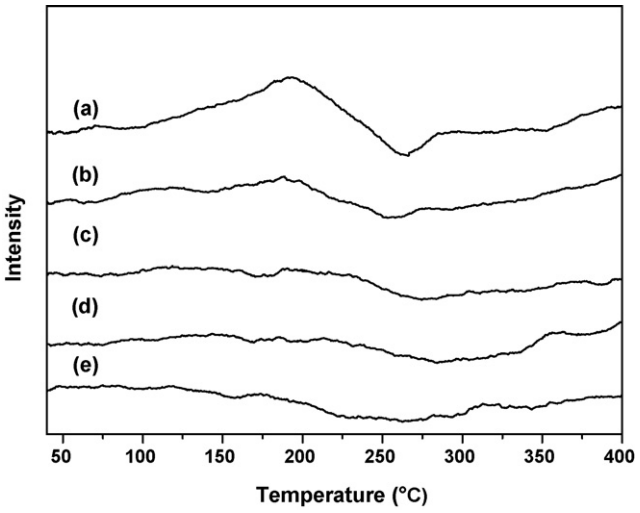

Fig. 4. O_2-TPD profiles of (a) CC-CP1, (b) CC-Im, (c) CC-CP2, (d) CC-Ct, and (e) CC-DE catalysts pretreated with N_2O. Pretreatment condition: the catalysts were pretreated under a flow of 2% N_2O/Ar at 400 °C for 1 h, followed by cooling down to room temperature in the same flow.

O_2-TPD profiles of the Co_3O_4–CeO_2 catalysts pretreated with N_2O. There was a broad and strong desorption peak around 200 °C over the CC-CP1 catalysts. The CC-Im catalyst showed a weak desorption peak at similar temperature. However, no obvious desorption peak was observed in the O_2-TPD profiles of the CC-CP2, CC-Ct, and CC-DE catalysts.

3.5. H_2-TPR measurements

According to the reaction mechanism (Eqs. (1) and (2)), the reducibility of Co^{3+} to Co^{2+} is a very important property for the decomposition of N_2O over cobalt containing catalysts. Therefore, H_2-TPR experiments were carried out to examine the reduction behavior of these Co_3O_4–CeO_2 catalysts. The TPR profiles are shown in Fig. 5. There were three well-defined reduction peaks in the profiles. The peak at 130 °C (P_{H_2}-I) is attributed to the reduction of surface oxygenated species. The other two peaks belong to the stepwise reduction of Co_3O_4 to metallic cobalt. According to the literature [21–26], the second reduction peak (P_{H_2}-II) centered at 250–350 °C is due to the reduction of Co^{3+} to Co^{2+}, and the third peak (P_{H_2}-III) at the region of 370–600 °C is due to the reduction of Co^{2+} to metallic cobalt Co^0 and partial reduction of Ce^{4+} to Ce^{3+}.

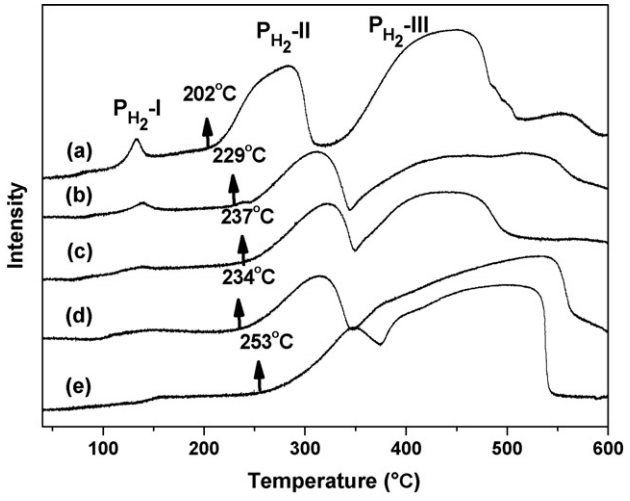

Fig. 5. H_2-TPR profiles of (a) CC-CP1, (b) CC-Im, (c) CC-CP2, (d) CC-Ct, and (e) CC-DE catalysts. The onset temperatures of P_{H_2}-II have been marked in the figure.

From these profiles, it can be seen that the reduction behavior of the catalyst is greatly influenced by the preparation method. The onset temperature of P_{H_2}-II, which represents the reducibility of Co^{3+} to Co^{2+}, was in the following order: CC-CP1 > CC-Im ≈ CC-Ct ≈ CC-CP2 > CC-DE as shown in Fig. 5. This sequence is similar to that of the catalytic activity, suggesting that the better the reducibility of Co^{3+} to Co^{2+}, the higher the catalytic activity of the Co_3O_4–CeO_2 catalyst for the decomposition of N_2O.

4. Discussion

4.1. Strong promotional effect of residual K on the catalytic activities of Co_3O_4–CeO_2 catalysts

According to their catalytic activities and characterization results, the five Co_3O_4–CeO_2 catalysts could be divided into two groups: Co_3O_4–CeO_2 catalysts with residual K (the CC-CP1, CC-Im, CC-CP2 catalysts) and Co_3O_4–CeO_2 catalysts without K (the CC-Ct, CC-DE catalysts).

The presence of a trace amount of K seemed to be very important for the decomposition of N_2O. Farris et al. [27] and Obalová et al. [28] have found that the presence of a residual Na remaining in the trace amount after a washing step could improve the activities of the mixed oxide catalysts co-precipitated by sodium precipitant. In this work, when ca. 0.7 mol% K was present on the surface of the catalyst (CC-CP2), the activity curve shifted dramatically to low temperatures compared to those of the catalysts without residual K. The CC-CP1 and CC-Im catalysts, which contained ca. 2 mol% K on the surface, showed better catalytic activities than the CC-CP2 catalyst. This result demonstrated that an appropriate amount of K in Co_3O_4–CeO_2 catalyst could improve the catalytic activity for N_2O decomposition reaction. When the amount of K in the catalyst was constant, the activity of the catalyst seemed to be related to its surface area. Table 3 summarized the specific activities, calculated by dividing the reaction rate of N_2O decomposition by BET surface area, over CC-CP1 and CC-Im catalysts at 200, 230 and 255 °C. The specific activities of these two catalysts were similar at these

Table 3
The specific activities per unit surface area over the CC-CP1 and CC-Im catalysts at different temperatures

Temperature (°C)	Specific activities of CC-CP1 ($molN_2O\ s^{-1}\ m^{-2}$)	Specific activities of CC-Im ($molN_2O\ s^{-1}\ m^{-2}$)
200	6.8×10^{-10}	7.68×10^{-10}
230	1.46×10^{-9}	1.59×10^{-9}
255	2.03×10^{-9}	2.57×10^{-9}

temperatures. However, the surface area of CC-CP1 was much larger than that of CC-Im. As a result, CC-CP1 showed the best activity by not only containing an appropriate amount of residual K but also having a large surface area.

When there was no K contained in the Co_3O_4–CeO_2 catalysts, the catalytic activity for the decomposition of N_2O decreased greatly. The difference between the catalytic activities of the CC-Ct and the CC-CP1 catalysts was great, even though these two catalysts had similar Co_3O_4 crystallite sizes, surface Ce/Co molar ratios, and surface areas. When Co_3O_4–CeO_2 catalyst was prepared by the direct evaporate method, the catalytic activity worsened because of the small surface area and the large crystallites.

It is reported that the doping of alkali metal to cobalt oxide catalysts can weaken the Co–O bond strength and promote oxygen desorption from Co_3O_4 [29]. A similar promotional effect may exist in these K containing catalysts in our study. It can be seen from the H_2-TPR experiment results (Fig. 5) that the reducibility of Co^{3+} to Co^{2+} in the CC-CP1 catalyst was greatly improved compared to other catalysts. This result is quite important, because N_2O decomposition is related to the reducibility of Co^{3+} to Co^{2+} (Eq. (2)). Therefore, the high catalytic activity of CC-CP1 could be well understood considering the high reducibility of Co species. Perez-Alonso et al. [30] have found the similar correlation of catalytic activity with TPR over $Fe_xCe_{1-x}O_2$ catalyst. In the present work, we supposed that the presence of K and the large surface area were the main factors for the best reducibility of CC-CP1. In addition, the low electronegativity of alkali metal may facilitate the electron transformation from an active site to the antibonding orbital of N_2O (Eq. (1)). For better understanding the promotion effect of alkali metals, more detailed work is now undergoing in our laboratory and will be present in a separate paper.

4.2. The rate-determining step of N_2O decomposition over Co_3O_4–CeO_2 catalysts

As stated in Section 3.4, the decomposition of N_2O proceeds by an oxidation–reduction mechanism (Eqs. (1) and (2)) [4]. The surface reaction of N_2O with the active site (Co^{2+} in Eq. (1)) is considered as a charge donation process from an active site into the antibonding orbital of N_2O, destabilizing the N–O bond and leading to the scission [4]. The adsorbed oxygen species left on the oxidized active site (Co^{3+}) may migrate on the surface, and desorb as a molecular oxygen through the combination of two such species concomitantly donating electrons back to Co^{3+} (Eq. (2)). Therefore, the redox ability of Co^{2+}/Co^{3+} is a very important indicator for the catalytic activity in N_2O decomposition.

In the O_2-TPD experiment of the catalyst pretreated with N_2O, there were strong and weak O_2 desorption peaks over the CC-CP1 and the CC-Im catalysts, respectively. However, no obvious O_2 desorption peak could be observed in the other three O_2-TPD profiles. There are two possibilities for the difference in O_2-TPD profiles. First, the active sites of the CC-CP2, CC-Ct and CC-DE catalysts are relatively inactive compared to those of the CC-CP1 and CC-Im catalysts. No decomposition of N_2O (Eq. (1)) can take place at low temperatures over these three catalysts. As a result, there is no oxygen species left on these catalysts. This assumption is in accordance with the activity test result. Second, the desorption of O_2 over the CC-CP2, CC-Ct, and CC-DE catalysts is very easy at low temperatures. Therefore, no oxygen species could be retained on the catalysts after the N_2O pretreatment process. To clarify the real process for the O_2 desorption result, we carried out an O_2-TPD experiment over the CC-Ct catalyst pretreated with O_2. Fig. 6 shows the comparison of O_2-TPD profiles of the CC-Ct catalyst pretreated with O_2 and N_2O, respectively. It can be seen from these profiles that there was a strong O_2 desorption peak when the catalyst was pretreated with O_2, which indicated that desorption of O_2 on this catalyst was not as easy as assumed in the second possibility. Therefore, the first possibility is the most reasonable explanation for the difference in O_2-TPD profiles of catalysts pretreated with N_2O. That means the active sites (Co^{2+}) of the CC-CP1 and CC-Im catalysts are more active than those of the other three catalysts.

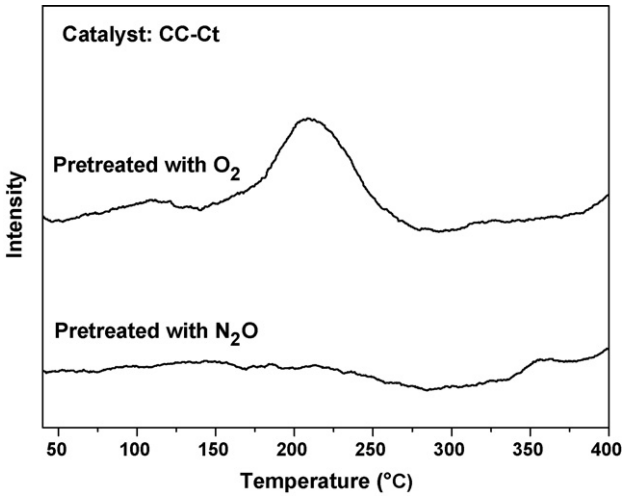

Fig. 6. O_2-TPD profiles of the CC-Ct catalyst pretreated with O_2 and N_2O, respectively. Pretreatment condition: the catalysts were pretreated under a flow of 10% O_2/He or 2% N_2O/Ar at 400 °C for 1 h, followed by cooling down to room temperature in the same flow.

The presence of O_2 desorption peaks of the CC-CP1 and CC-Im catalysts also suggests that the surface reaction of N_2O with Co^{2+} (Eq. (1)) is relatively easier than the desorption of O_2 (Eq. (2)). Thus the desorption of O_2 is thought to be the rate-determining step of the reaction over these two catalysts. As little O_2 desorption could be observed over the CC-CP2, CC-Ct and CC-DE catalysts, the surface reaction of N_2O (Eq. (1)) should be the rate-determining step over these catalysts. Considering all these discussions about rate-determining step are based on the O_2-TPD results, the conclusions are reasonable below the temperature of O_2 desorption. When reaction temperatures are higher than the temperature of O_2 desorption, it is hard to discuss the rate-determining step from the present O_2-TPD results. Additional work is needed for further discussion.

5. Conclusions

The Co_3O_4–CeO_2 catalyst prepared by the co-precipitation method with K_2CO_3 as precipitant (CC-CP1) exhibited the best

catalytic performance for the decomposition of N_2O, followed by that prepared by the impregnation method (CC-Im) and the co-precipitation method with KOH as the precipitant (CC-CP2). The Co_3O_4–CeO_2 catalyst prepared by the citrate method (CC-Ct) and, to a greater extent, that prepared by the direct evaporation method (CC-DE) exhibited relatively poorer catalytic performance.

The redox properties of Co^{2+}/Co^{3+} may be improved when there is residual K in the Co_3O_4–CeO_2 catalysts. The presence of ca. 2 mol% residual K on the surface and the large surface area are thought to be the main reasons for the best catalytic activity for decomposition of N_2O over the CC-CP1 catalyst. From the O_2-TPD experiment results, we propose that at low temperatures the oxygen desorption step (Eq. (2)) is the rate-determining step of the whole decomposition reaction over the CC-CP1 and CC-Im catalysts. The surface reaction of N_2O with the active site (Eq. (1)) is postulated to be the rate-determining step over the CC-CP2, CC-Ct, and CC-DE catalysts at low temperatures.

Acknowledgements

This work was financially supported by the National Natural Science Foundation of China (20425722, 20621140004) and the Ministry of Science and Technology, China (2004CB719503).

References

[1] M.H. Thiemens, W.C. Trogler, Science 251 (1991) 932.
[2] W.C. Trogler, Coord. Chem. Rev. 187 (1999) 303.
[3] J. Pérez-Ramírez, F. Kapteijn, K. Schöffel, J.A. Moulijn, Appl. Catal. B 44 (2003) 117.
[4] F. Kapteijn, J. Rodriguez-Mirasol, J.A. Moulijn, Appl. Catal. B 9 (1996) 25.
[5] K. Yuzaki, T. Yarimizu, K. Aoyagi, S.-I. Ito, K. Kunimori, Catal. Today 45 (1998) 129.
[6] L. Yan, X. Zhang, T. Ren, H. Zhang, X. Wang, J. Suo, Chem. Commun. (2002) 860.
[7] K. Doi, Y.Y. Wu, R. Takeda, A. Matsunami, N. Arai, T. Tagawa, S. Goto, Appl. Catal. B 35 (2001) 43.
[8] J. Pérez-Ramírez, F. Kapteijn, G. Mul, X. Xu, J.A. Moulijn, Catal. Today 76 (2002) 55.
[9] J. Pérez-Ramírez, F. Kapteijn, Appl. Catal. B 47 (2004) 177.
[10] R. Sundararajan, V. Srinivasan, Appl. Catal. 73 (1991) 165.
[11] J.N. Armor, T.A. Braymer, T.S. Farris, Y. Li, F.P. Petrocelli, E.L. Weist, S. Kannan, C.S. Swamy, Appl. Catal. B 7 (1996) 397.
[12] S. Kannan, Appl. Clay Sci. 13 (1998) 347.
[13] S. Kannan, C.S. Swamy, Catal. Today 53 (1999) 725.
[14] J. Pérez-Ramírez, J. Overeijnder, F. Kapteijn, J.A. Moulijn, Appl. Catal. B 23 (1999) 59.
[15] U. Chellam, Z.P. Xu, H.C. Zeng, Chem. Mater. 12 (2000) 650.
[16] L. Yan, T. Ren, X. Wang, Q. Gao, D. Ji, J. Suo, Catal. Commun. 4 (2003) 505.
[17] L. Yan, T. Ren, X. Wang, D. Ji, J. Suo, Appl. Catal. B 45 (2003) 85.
[18] L. Xue, C. Zhang, H. He, Y. Teraoka, Appl. Catal. B 75 (2007) 157.
[19] J.-G. Kim, D.L. Pugmire, D. Battaglia, M.A. Langell, Appl. Surf. Sci. 165 (2000) 70.
[20] C.D. Wagner, W.M. Riggs, L.E. Davis, J.F. Moulder, G.E. Muilenberg (Eds.), Handbook of X-ray Photoelectron Spectroscopy, Physical Electronics Division, Perkin-Elmer Corporation., (1979).
[21] S. Damyanova, C.A. Perez, M. Schmal, J.M.C. Bueno, Appl. Catal. A 234 (2002) 271.
[22] S. Damyanova, J.M.C. Bueno, Appl. Catal. A 253 (2003) 135.
[23] L.F. Liotta, G.D. Carlo, G. Pantaleo, A.M. Venezia, G. Deganello, Appl. Catal. B 66 (2006) 217.
[24] P.G. Harrison, I.K. Ball, W. Daniell, P. Lukinskas, M. Céspedes, E.E. Miró, M.A. Ulla, Chem. Eng. J. 95 (2003) 47.
[25] N. Bahlawane, E.F. Rivera, K. Kohse-Höinghaus, A. Brechling, U. Kleineberg, Appl. Catal. B 53 (2004) 245.
[26] H.-Y. Lin, Y.-W. Chen, Mater. Chem. Phys. 85 (2004) 171.
[27] T.S. Farris, Y. Li, J.N. Armor, T.A. Braymer, US Patent 5,472,677 (1995), to Engelhard Corporation.
[28] L. Obalová, K. Jirátová, F. Kovanda, M. Valášková, J. Balabánová, K. Pacultová, J. Mol. Catal. A 248 (2006) 210.
[29] M. Haneda, Y. Kintaichi, N. Bion, H. Hamada, Appl. Catal. B 46 (2003) 473.
[30] F.J. Perez-Alonso, I. Melián-Cabrera, M.L. Granados, F. Kapteijn, J.L.G. Fierro, J. Catal. 239 (2006) 340.